A Rigorous Analytical Solution to Abrupt Dielectric Waveguide Discontinuities

Nagayoshi Morita, *Senior Member, IEEE*

Abstract—**A simple analytical method is proposed for analyzing transmitted, reflected, and radiated fields in abrupt discontinuities of dielectric waveguides, such as step discontinuities and sharp bends. In this method, approximate transmitted fields, both guided mode fields and radiated fields, are first calculated by assuming the incident field to be the source field on the discontinuity interface. Next, the approximate reflected fields are calculated by assuming the difference field of the incident and approximate transmitted fields to be the source field on the discontinuity interface. Then, the improvements for these approximate transmitted fields and approximate reflected fields are calculated in turns, successively. Only a few successive steps suffice for obtaining rigorous solutions. Numerical examples are presented for step discontinuities and sharp bends of dielectric slab waveguides.**

I. Introduction

A great many papers have been published on abrupt discontinuities of dielectric waveguides. A fair number of these papers are listed in [1] and [4]. Almost all of these papers aim at full-wave analysis and therefore resort necessarily to certain numerical techniques, except for a few of the earlier papers.

Going against the trend of developing better numerical techniques, this paper shows that a new, simple analytical method can be successfully constructed for obtaining rigorous solutions to the problem of abrupt discontinuities of dielectric waveguides. Although the method employs a successive process, it is ensured theoretically that the solution series converges very rapidly, which is essentially different from the successive solutions to the integral equations for the boundary conditions that were used in [1]–[3].

The theory is applied to the step discontinuities and sharp bends. Rigorous values are presented of transmitted guided mode power, transmitted radiated power, reflected guided mode power, reflected radiated power, radiation pattern, etc. These results serve for the purpose of checking the accuracy of various numerical methods that are being planned or are under study.

Manuscript received September 6, 1990; revised March 21, 1991.

The author was with the Faculty of Engineering, Osaka University, Osaka, Japan. He is now with the Department of Electrical Engineering, Chiba Institute of Technology, Narashino, Chiba 275, Japan.

IEEE Log Number 9101024.

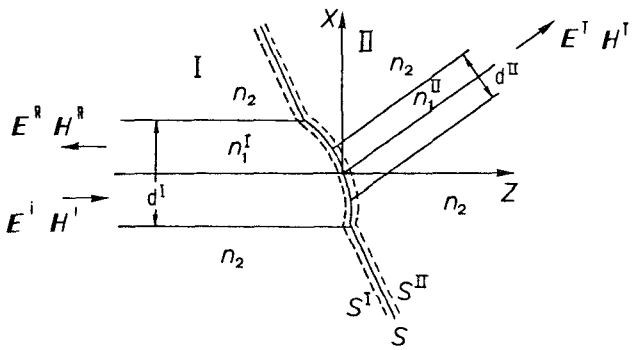

Fig. 1. Abrupt discontinuity of dielectric slab waveguide

II. Theory

A. Successive Calculation of Transmitted and Reflected Fields

Consider the abrupt discontinuity of Fig. 1, in which slab waveguide I with core width d^{I} and core refractive index n_1^{I} and slab waveguide II with core width d^{II} and core refractive index n_1^{II} are connected at a surface S; both waveguides I and II have the same cladding refractive index, n_2. Let the electromagnetic fields $\boldsymbol{E}^i, \boldsymbol{H}^i$ be incident on S from the side of waveguide I (or simply "side I") and let the transmitted fields and reflected fields be $\boldsymbol{E}^T, \boldsymbol{H}^T$ and $\boldsymbol{E}^R, \boldsymbol{H}^R$, respectively. The surfaces S^{I} and S^{II} are defined to be the surfaces that are very close to S in the sides I and II, respectively.

First we assume on S^{II} those electromagnetic field sources whose tangential components are identical to the tangential components of the incident fields, $\boldsymbol{E}_t^i, \boldsymbol{H}_t^i$, where the subscript t denotes the tangential component. Then we name the fields on the side II produced by these sources the first-order transmitted electromagnetic fields and express these as $\boldsymbol{E}^{T(1)}, \boldsymbol{H}^{T(1)}$. If the tangential components of $\boldsymbol{E}^{T(1)}$ and $\boldsymbol{H}^{T(1)}$ on S, $\boldsymbol{E}_t^{T(1)}$ and $\boldsymbol{H}_t^{T(1)}$, are just equal to $\boldsymbol{E}_t^i$ and $\boldsymbol{H}_t^i$, respectively, on S, the reflected fields on side I must be null. However, this situation never happens as long as there exists some discontinuity at S between the left and right sides. Thus, we consider that the differences between the first-order transmitted fields and the incident fields on S act as sources for the fields reflected back to side I. That is, we next assume the following tangential electromagnetic field sources $\delta \boldsymbol{E}^{(1)}$

0018-9480/91/0800-1272$01.00 ©1991 IEEE

and $\delta \boldsymbol{H}^{(1)}$ on S^{I}:

$$\delta \boldsymbol{E}_t^{(1)} = \boldsymbol{E}_t^{T(1)} - \boldsymbol{E}_t^i \qquad \delta \boldsymbol{H}_t^{(1)} = \boldsymbol{H}_t^{T(1)} - \boldsymbol{H}_t^i. \tag{1}$$

In this assumption, the equality between the tangential components of fields on S^{II} and those on S^{I} is tacitly used. We name the fields on side I produced by the sources $\delta \boldsymbol{E}_t^{(1)}$ and $\delta \boldsymbol{H}_t^{(1)}$ the first-order reflected fields and express them as $\boldsymbol{E}^{R(1)}, \boldsymbol{H}^{R(1)}$. Since the incident fields $\boldsymbol{E}^i, \boldsymbol{H}^i$ on S^{I} do not contribute to the reflected fields on side I, it follows that only $\boldsymbol{E}_t^{T(1)}, \boldsymbol{H}_t^{T(1)}$ of the right-hand side of (1) act as the sources of $\boldsymbol{E}^{R(1)}, \boldsymbol{H}^{R(1)}$.

As a matter of course, the tangential components of $\boldsymbol{E}^{R(1)}$ and $\boldsymbol{H}^{R(1)}$ on S^{I} do not coincide with the corresponding fields on S^{I}, $\delta \boldsymbol{E}_t^{(1)}$ and $\delta \boldsymbol{H}_t^{(1)}$. Therefore, we further assume as the sources on S^{II} the following tangential components of the difference field between $\boldsymbol{E}^{R(1)}$ and $\delta \boldsymbol{E}^{(1)}$ and the difference field between $\boldsymbol{H}^{R(1)}$ and $\delta \boldsymbol{H}^{(1)}$:

$$\begin{aligned} \delta \boldsymbol{E}_t^{(2)} &= \boldsymbol{E}_t^{R(1)} - \delta \boldsymbol{E}_t^{(1)} = \boldsymbol{E}_t^{R(1)} - \left(\boldsymbol{E}_t^{T(1)} - \boldsymbol{E}_t^i\right) \\ \delta \boldsymbol{H}_t^{(2)} &= \boldsymbol{H}_t^{R(1)} - \delta \boldsymbol{H}_t^{(1)} = \boldsymbol{H}_t^{R(1)} - \left(\boldsymbol{H}_t^{T(1)} - \boldsymbol{H}_t^i\right). \end{aligned} \tag{2}$$

We name the fields produced on side II by $\delta \boldsymbol{E}_t^{(2)}, \delta \boldsymbol{H}_t^{(2)}$ on S^{II} the second-order transmitted fields and express them as $\boldsymbol{E}^{T(2)}, \boldsymbol{H}^{T(2)}$. It is clear that the fields on side II caused by the source fields $\delta \boldsymbol{E}_t^{(1)}$ and $\delta \boldsymbol{H}_t^{(1)}$ become zero because these fields are already taken into account when the first-order transmitted fields are calculated. (Refer to (1).) It follows, therefore, that only $\boldsymbol{E}_t^{R(1)}, \boldsymbol{H}_t^{R(1)}$ of the right-hand side of (2) contribute to producing the fields $\boldsymbol{E}^{T(2)}, \boldsymbol{H}^{T(2)}$. In similar fashion, we define the nth-order reflected electromagnetic fields, $\boldsymbol{E}^{R(n)}, \boldsymbol{H}^{R(n)}$, and the $(n+1)$th-order transmitted electromagnetic fields, $\boldsymbol{E}^{T(n+1)}, \boldsymbol{H}^{T(n+1)}$ $(n = 2, 3, \cdots)$. Then, it follows that only the source fields $\boldsymbol{E}_t^{T(n)}, \boldsymbol{H}_t^{T(n)}$ on S^{I} produce $\boldsymbol{E}^{R(n)}, \boldsymbol{H}^{R(n)}$ and that only the source fields $\boldsymbol{E}_t^{R(n)}, \boldsymbol{H}_t^{R(n)}$ on S^{II} produce $\boldsymbol{E}^{T(n+1)}, \boldsymbol{H}^{T(n+1)}$.

As is clear from the successive steps explained above, the source of the nth-order transmitted fields on side II is the yet-mismatched quantity, on the surface S, between the tangential components of the reflected fields down to the $(n-1)$th order and those of the transmitted fields down to the $(n-1)$th order; the source of the nth-order reflected fields on side I is the yet-mismatched quantity, on the surface S, between the tangential components of the reflected fields down to the $(n-1)$th order and those of the transmitted fields down to the nth order. Therefore, the higher order transmitted and reflected fields rapidly decreases as the mismatched field quantity decreases. In other words, the transmitted and reflected electromagnetic fields, $\boldsymbol{E}_N^T, \boldsymbol{H}_N^T$ and $\boldsymbol{E}_N^R, \boldsymbol{H}_N^R$, given by

$$\boldsymbol{E}_N^T = \sum_{n=1}^{N} \boldsymbol{E}^{T(n)} \qquad \boldsymbol{H}_N^T = \sum_{n=1}^{N} \boldsymbol{H}^{T(n)} \tag{3}$$

$$\boldsymbol{E}_N^R = \sum_{n=1}^{N} \boldsymbol{E}^{R(n)} \qquad \boldsymbol{H}_N^R = \sum_{n=1}^{N} \boldsymbol{H}^{R(n)} \tag{4}$$

rapidly converge to the true transmitted fields $\boldsymbol{E}^T, \boldsymbol{H}^T$ and the true reflected fields $\boldsymbol{E}^R, \boldsymbol{H}^R$, respectively, with the increase of N. It is evident that $|\boldsymbol{E}^{T(n+1)}| < |\boldsymbol{E}^{R(n)}| < |\boldsymbol{E}^{T(n)}|$ and $|\boldsymbol{E}^{R(n+1)}| < |\boldsymbol{E}^{T(n+1)}| < |\boldsymbol{E}^{R(n)}|$ hold, or rather, in most cases $|\boldsymbol{E}^{T(n+1)}/\boldsymbol{E}^{T(n)}| \ll 1$ and $|\boldsymbol{E}^{R(n+1)}/\boldsymbol{E}^{R(n)}| \ll 1$. Therefore, the rate of convergence of the series (3) and (4) is remarkably high and moreover they converge absolutely.

B. Mode Expressions of Reflected and Transmitted Fields

We express electromagnetic fields in dielectric waveguide regions $(\boldsymbol{E}, \boldsymbol{H})$ in terms of mode fields for the dielectric waveguide $(\underline{\boldsymbol{E}}, \underline{\boldsymbol{H}})$ as follows:

$$\boldsymbol{E} = \sum_m a_m \underline{\boldsymbol{E}}_m + \int b(\Gamma)\, \underline{\boldsymbol{E}}(\Gamma)\, d\Gamma \tag{5}$$

$$\boldsymbol{H} = \sum_m a_m \underline{\boldsymbol{H}}_m + \int b(\Gamma)\, \underline{\boldsymbol{H}}(\Gamma)\, d\Gamma \tag{6}$$

where the first terms on the right-hand sides of (5) and (6) are the sums of the guided modes, and the second terms are the spectral integrals of the radiation modes, and these mode fields are written as

$$\underline{\boldsymbol{E}}_m = \boldsymbol{e}_m e^{-j\beta_m z} \qquad \underline{\boldsymbol{H}}_m = \boldsymbol{h}_m e^{-j\beta_m z} \tag{7}$$

$$\underline{\boldsymbol{E}}(\Gamma) = \boldsymbol{e}(\Gamma) e^{-j\beta z} \qquad \underline{\boldsymbol{H}}(\Gamma) = \boldsymbol{h}(\Gamma) e^{-j\beta z} \tag{8}$$

where β_m is the propagation constant in the z direction of guided modes and the subscript m denotes a guided mode number. β and Γ are the wavenumbers with respect to radiation modes; β is the wavenumber in the z direction and Γ is that in the x direction in the cladding region, the relation between them being $\Gamma = (n_2^2 k_0^2 - \beta^2)^{1/2}$, where k_0 denotes the free-space wavenumber. The specific expressions for $\boldsymbol{e}_m$, $\boldsymbol{h}_m$, $\boldsymbol{e}(\Gamma)$, and $\boldsymbol{h}(\Gamma)$ are given, for example, in [5] for both TE and TM modes. The range of integration of Γ in (5) and (6) is usually 0 to ∞. Rigorously, however, when the real value range of β is not 0 to k_0 but a certain value α to k_0 or $-\alpha$ to k_0, the range of Γ should be modified to exclude or include the spectral range corresponding to $\beta = 0$ to α or $\beta = -\alpha$ to 0. This case occurs, for instance, when the fields are those which emanate from a tilted surface S. This modification, however, is not very important in most practical numerical calculations for the present problem of waveguide discontinuities, since the power included in the modified part of the spectrum is, in most cases, negligibly small.

Next, we explain how to get the transmitted fields $\boldsymbol{E}^{\mathrm{II}}, \boldsymbol{H}^{\mathrm{II}}$ when source fields $\boldsymbol{E}_t^0, \boldsymbol{H}_t^0$ are given on surface S^{II}. Fig. 2 shows a cross section of the part of waveguide II on the right side of the junction. The configuration is assumed to be uniform in the y direction. Let C_0 be the line which lies in the cross section of Fig. 2 and which is on S^{II}, let C_f be the straight line parallel to the x axis a certain distance from C_0, and let $C_\infty^{(+)}$ and $C_\infty^{(-)}$ be the straight lines parallel to the z axis and at $x = +\infty$ and $x = -\infty$, respectively. It is convenient to assign the directions to these lines as shown in Fig. 2 using arrows. Also, let the three regions bounded by the lines $C_\infty^{(+)}$, C_0, $C_\infty^{(-)}$,

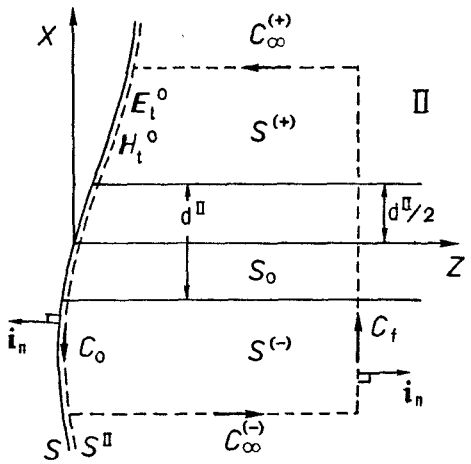

Fig. 2. A cross section of the part of waveguide II.

and C_f and the core–cladding boundary lines $x = d^{II}/2$ and $x = -d^{II}/2$ be $S^{(+)}$, S_0, and $S^{(-)}$ as in Fig. 2.

First, the transmitted fields $\boldsymbol{E}^{II}, \boldsymbol{H}^{II}$ are expressed in terms of the mode fields in waveguide II, i.e., $\underline{\boldsymbol{E}}^{II}, \underline{\boldsymbol{H}}^{II}$ ($\underline{\boldsymbol{E}}_m^{II}$, $\underline{\boldsymbol{H}}_m^{II}$ or $\underline{\boldsymbol{E}}^{II}(\Gamma), \underline{\boldsymbol{H}}^{II}(\Gamma)$), in the form of (5) and (6). Then, applying the Lorentz reciprocity theorem for the field pairs $\boldsymbol{E}^{II}$, $\boldsymbol{H}^{II}$ and $\underline{\boldsymbol{E}}^{II}, \underline{\boldsymbol{H}}^{II}$ in each region of $S^{(+)}$, S_0, and $S^{(-)}$ and adding the three results, we have zero values for the integrals on the regions $S^{(+)}$, S_0, and $S^{(-)}$ because there are no sources within these regions. Also, we have zero values for the integrals on the lines $x = \pm d^{II}/2$ and the lines $C_\infty^{(+)}$ and $C_\infty^{(-)}$ because of the boundary conditions on $x = \pm d^{II}/2$ and the radiation condition of $\boldsymbol{E}^{II}, \boldsymbol{H}^{II}$ at $x = \pm\infty$, respectively, the result being

$$\int_{C_f} \left(\underline{\boldsymbol{E}}^{II} \times \boldsymbol{H}^{II*} + \boldsymbol{E}^{II*} \times \underline{\boldsymbol{H}}^{II}\right) \cdot \boldsymbol{i}_n \, dl + \int_{C_0} \left(\underline{\boldsymbol{E}}^{II} \times \boldsymbol{H}_t^{0*} + \boldsymbol{E}_t^{0*} \times \underline{\boldsymbol{H}}^{II}\right) \cdot \boldsymbol{i}_n \, dl = 0 \quad (9)$$

where $\boldsymbol{i}_n$ is the outwardly directed unit normal and $*$ denotes the complex conjugate. If β^{II} is imaginary, mode fields $\underline{\boldsymbol{E}}^{II}, \underline{\boldsymbol{H}}^{II}$ must be replaced by those which propagate in the negative z direction. If guided mode fields $\underline{\boldsymbol{E}}_m^{II}, \underline{\boldsymbol{H}}_m^{II}$ are used for $\underline{\boldsymbol{E}}^{II}, \underline{\boldsymbol{H}}^{II}$ in (9), the normalized orthogonality properties for the guided modes

$$\frac{1}{2}\int_{-\infty}^{\infty} (\boldsymbol{e}_m \times \boldsymbol{h}_n^*) \cdot \boldsymbol{i}_z \, dx = \delta_{mn} \quad (10)$$

can be used to derive from the integral on C_f of (9) the expansion coefficients a_m, where δ_{mn} denotes the Kronecker delta function. In this case, we have from (9)

$$a_m = -\frac{1}{4}\int_{C_0} \left(\underline{\boldsymbol{E}}_m^{II*} \times \boldsymbol{H}_t^0 + \boldsymbol{E}_t^0 \times \underline{\boldsymbol{H}}_m^{II*}\right) \cdot \boldsymbol{i}_n \, dl. \quad (11)$$

On the other hand, if radiation mode fields $\underline{\boldsymbol{E}}^{II}(\Gamma), \underline{\boldsymbol{H}}^{II}(\Gamma)$ are chosen as $\underline{\boldsymbol{E}}^{II}, \underline{\boldsymbol{H}}^{II}$ in (9), the normalized orthogonality properties for the radiation modes

$$\frac{1}{2}\int_{-\infty}^{\infty} \left(\boldsymbol{e}(\Gamma_p) \times \boldsymbol{h}^*(\Gamma_q)\right) \cdot \boldsymbol{i}_z \, dx = \begin{cases} (\beta_p^*/|\beta_p|)\delta(\Gamma_p - \Gamma_q), & \text{TE radiation modes} \\ (\beta_p/|\beta_p|)\delta(\Gamma_p - \Gamma_q), & \text{TM radiation modes} \end{cases} \quad (12)$$

can be used to derive from the integral on C_f the expansion coefficient $b(\Gamma)$, where $\delta(\ )$ is the Dirac delta function. In this case, we have from (9)

$$b(\Gamma) = -\frac{1}{4}\int_{C_0} \left(\underline{\boldsymbol{E}}^{II}(\Gamma)^* \times \boldsymbol{H}_t^0 + \boldsymbol{E}_t^0 \times \underline{\boldsymbol{H}}^{II}(\Gamma)^*\right) \cdot \boldsymbol{i}_n \, dl \quad (13)$$

for real β^{II}, and for imaginary β^{II}

$$b(\Gamma) = -\frac{ju_s}{4}\int_{C_0} \left(\underline{\bar{\boldsymbol{E}}}^{II}(\Gamma)^* \times \boldsymbol{H}_t^0 + \boldsymbol{E}_t^0 \times \underline{\bar{\boldsymbol{H}}}^{II}(\Gamma)^*\right) \cdot \boldsymbol{i}_n \, dl. \quad (14)$$

Here u_s is $+1$ or -1, depending on whether $\underline{\boldsymbol{E}}^{II}(\Gamma), \underline{\boldsymbol{H}}^{II}(\Gamma)$ are TE-mode fields or TM-mode fields, and the fields marked with overbars ($\underline{\bar{\boldsymbol{E}}}^{II}, \underline{\bar{\boldsymbol{H}}}^{II}$) denote the radiation mode fields propagating in the negative z direction. We can obtain analogously the mode expansion coefficients for the fields produced in side I when sources are given on S^I just to the left of surface S. The results are similar to (11), (13), and (14) and are omitted here.

Now, it is very easy to get the expansion coefficients a_m and $b(\Gamma)$ for the fields of waveguide II expressed in the form of (5) and (6) when the source fields on C_0, i.e., $\boldsymbol{E}_t^0$ and $\boldsymbol{H}_t^0$, are given in terms of the mode fields of waveguide I that propagate in the negative z direction. Let $\boldsymbol{E}_t^0, \boldsymbol{H}_t^0$ be given by

$$\boldsymbol{E}_t^0 = \sum c_m \underline{\bar{\boldsymbol{E}}}_{tm}^I + \int g(\Gamma)\, \underline{\bar{\boldsymbol{E}}}_t^I(\Gamma)\, d\Gamma \quad (15)$$

$$\boldsymbol{H}_t^0 = \sum c_m \underline{\bar{\boldsymbol{H}}}_{tm}^I + \int g(\Gamma)\, \underline{\bar{\boldsymbol{H}}}_t^I(\Gamma)\, d\Gamma. \quad (16)$$

Then, substituting (15) and (16) into (11), (13), and (14) yields the following three expressions:

$$a_m = \frac{1}{2}\left\{ \sum \left(a'^I_{m'm} + a''^I_{m'm}\right) c_{m'} + \int \left(\bar{b}'_m(\Gamma)^I + \bar{b}''_m(\Gamma)^I\right) g(\Gamma)\, d\Gamma \right\} \quad (17)$$

$$b(\Gamma) = \frac{1}{2}\left\{ \sum_{m'} \left(b'_{m'}(\Gamma)^I + b''_{m'}(\Gamma)^I\right) c_{m'} + \int \left(g'(\Gamma', \Gamma)^I + g''(\Gamma', \Gamma)^I\right) g(\Gamma')\, d\Gamma' \right\} \quad (18)$$

for real β^{II}, and

$$b(\Gamma) = \frac{ju_s}{2}\left\{\sum_{m'}\left(b'_{m'}(\Gamma)^{I,II} + b''_{m'}(\Gamma)^{I,II}\right)c_{m'} + \int\left(g'(\Gamma',\Gamma)^{I,II} + g''(\Gamma',\Gamma)^{I,II}\right)g(\Gamma')\,d\Gamma'\right\} \quad (19)$$

for imaginary β^{II}, where

$$a'_{mm'} = -\frac{1}{2}\int_{C_0}\left(\underline{E}^{I}_{tm}\times\underline{H}^{II*}_{tm'}\right)\cdot i_n\,dl \quad (20)$$

$$a''_{mm'} = -\frac{1}{2}\int_{C_0}\left(\underline{E}^{II*}_{tm'}\times\underline{H}^{I}_{tm}\right)\cdot i_n\,dl \quad (21)$$

$$b'_m(\Gamma) = -\frac{1}{2}\int_{C_0}\left(\underline{E}^{I}_{tm}\times\underline{H}^{II}_{t}(\Gamma)^*\right)\cdot i_n\,dl \quad (22)$$

$$b''_m(\Gamma) = -\frac{1}{2}\int_{C_0}\left(\underline{E}^{II}_{t}(\Gamma)^*\times\underline{H}^{I}_{tm}\right)\cdot i_n\,dl \quad (23)$$

$$\bar{b}'_m(\Gamma) = -\frac{1}{2}\int_{C_0}\left(\underline{E}^{I}_{t}(\Gamma)\times\underline{H}^{II*}_{tm}\right)\cdot i_n\,dl \quad (24)$$

$$\bar{b}''_m(\Gamma) = -\frac{1}{2}\int_{C_0}\left(\underline{E}^{II*}_{tm}\times\underline{H}^{I}_{t}(\Gamma)\right)\cdot i_n\,dl \quad (25)$$

$$g'(\Gamma,\Gamma') = -\frac{1}{2}\int_{C_0}\left(\underline{E}^{I}_{t}(\Gamma)\times\underline{H}^{II}_{t}(\Gamma')^*\right)\cdot i_n\,dl \quad (26)$$

$$g''(\Gamma,\Gamma') = -\frac{1}{2}\int_{C_0}\left(\underline{E}^{II}_{t}(\Gamma')^*\times\underline{H}^{I}_{t}(\Gamma)\right)\cdot i_n\,dl. \quad (27)$$

The superscripts I and II on $a'_{m'm}, b'_{m'}(\Gamma)$, etc., mean that the signs of the propagation constants β^{I} and β^{II} are changed in the expressions without those symbols, depending on whether I or II is attached. In the special case where $\boldsymbol{E}^0_t, \boldsymbol{H}^0_t$ on C_0 are the m'th guided mode fields of waveguide I with amplitude $C_{m'}$ propagating in the positive z direction, the expansion coefficients (17)–(19) reduce to the following simpler forms:

$$a_m = \frac{1}{2}\left(a'_{m'm} + a''_{m'm}\right)c_{m'} \quad (28)$$

$$b(\Gamma) = \frac{1}{2}\left(b'_{m'}(\Gamma) + b''_{m'}(\Gamma)\right)c_{m'}, \quad \text{for real } \beta^{II} \quad (29)$$

$$= -\frac{ju_s}{2}\left(b'_{m'}(\Gamma) - b''_{m'}(\Gamma)\right)c_{m'}, \quad \text{for imaginary } \beta^{II}. \quad (30)$$

Similarly, we can obtain the fields $\boldsymbol{E}^{I}, \boldsymbol{H}^{I}$ on side I produced by those source fields on S^{I} just to the left of surface S whose tangential components are expressed by

$$\boldsymbol{E}^0_t = \sum_m a_m\underline{E}^{II}_{tm} + \int b(\Gamma)\underline{E}^{II}_{t}(\Gamma)\,d\Gamma \quad (31)$$

$$\boldsymbol{H}^0_t = \sum_m a_m\underline{H}^{II}_{tm} + \int b(\Gamma)\underline{H}^{II}_{t}(\Gamma)\,d\Gamma. \quad (32)$$

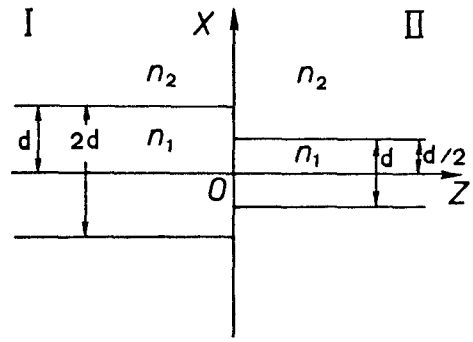

Fig. 3. Step discontinuity.

That is, the mode expansion forms for $\boldsymbol{E}^{I}, \boldsymbol{H}^{I}$ are given by

$$\boldsymbol{E}^{I} = \sum_m c_m\bar{\underline{E}}^{I}_m + \int g(\Gamma)\bar{\underline{E}}^{I}(\Gamma)\,d\Gamma \quad (33)$$

$$\boldsymbol{H}^{I} = \sum_m c_m\bar{\underline{H}}^{I}_m + \int g(\Gamma)\bar{\underline{H}}^{I}(\Gamma)\,d\Gamma \quad (34)$$

where the expansion coefficients c_m and $g(\Gamma)$ become

$$c_m = -\frac{1}{2}\left\{\sum_{m'}\left(a'^{I*}_{mm'} + a''^{I*}_{mm'}\right)a_{m'} + \int\left(b'_m(\Gamma)^{I*} + b''_m(\Gamma)^{I*}\right)b(\Gamma)\,d\Gamma\right\} \quad (35)$$

$$g(\Gamma) = -\frac{1}{2}\left\{\sum_{m'}\left(\bar{b}'_{m'}(\Gamma)^{I*} + \bar{b}''_{m'}(\Gamma)^{I*}\right)a_{m'} + \int\left(g'(\Gamma,\Gamma')^{I*} + g''(\Gamma,\Gamma')^{I*}\right)b(\Gamma')\,d\Gamma'\right\} \quad (36)$$

for real β^{I} and

$$g(\Gamma) = -\frac{ju_s}{2}\left\{\sum_{m'}\left(\bar{b}'_{m'}(\Gamma)^* + \bar{b}''_{m'}(\Gamma)^*\right)a_{m'} + \int\left(g'(\Gamma,\Gamma')^* + g''(\Gamma,\Gamma')^*\right)b(\Gamma')\,d\Gamma'\right\} \quad (37)$$

for imaginary β^{I}.

III. Numerical Examples

A. Step Discontinuities

The step discontinuity configuration treated here is shown in Fig. 3. The core widths of waveguides I and II are $2d$ and d, respectively, and the refractive indices of the core and cladding are n_1 and n_2 for both waveguides. The incident field is assumed to be the TE_0 mode with unit power, incident on the junction at $z = 0$ from the side of waveguide I. The first-order transmitted field, the first-order reflected field, and the second-order transmitted field were calculated using the equations presented in the previous section for eight cases, four for the case of small refractive index difference, i.e., $n_1 = 1.01$ and $n_2 = 1.0$, and four for the case of relatively large refractive index difference, i.e., $n_1 = 1.432$ and $n_2 = 1.0$. The power

TABLE I
REFLECTED AND TRANSMITTED POWER ($n_1 = 1.01$, $n_2 = 1.0$)

k_0d		5.0	10.0	20.0	40.0
$P^{T(1)}$	Guided	0.94392	0.98995	0.95718	0.86334
	Radiation	0.56085×10^{-1}	0.10065×10^{-1}	0.42827×10^{-1}	0.13666
	Total	1.00001	1.00001	1.00001	1.00001
$P^{R(1)}$	Guided	0.13486×10^{-5}	0.25987×10^{-5}	0.23507×10^{-5}	0.16739×10^{-5} 0.30990×10^{-5}
	Radiation	0.98447×10^{-5}	0.79565×10^{-5}	0.59923×10^{-5}	0.18661×10^{-5}
	Total	0.11193×10^{-4}	0.10555×10^{-4}	0.83430×10^{-5}	0.66390×10^{-5}
$P^{T(1)}+P^{R(1)}$		1.00002	1.00002	1.00002	1.00002
$P^{T(2)}$	Guided	0.59260×10^{-10}	0.83594×10^{-10}	0.28565×10^{-10}	0.58026×10^{-11}
	Radiation	0.64853×10^{-9}	0.80739×10^{-9}	0.10126×10^{-8}	0.12346×10^{-8}
	Total	0.70779×10^{-9}	0.89099×10^{-9}	0.10412×10^{-8}	0.12404×10^{-8}
$P^{T(1+2)}$	Guided	0.94391	0.98993	0.95717	0.86334
	Radiation	0.56082×10^{-1}	0.10063×10^{-1}	0.42823×10^{-1}	0.13666
	Total	0.99999	0.99999	0.99999	0.99999
$P^{T(1+2)}+P^{R(1)}$		1.00000	1.00000	1.00000	1.00000

TABLE II
REFLECTED AND TRANSMITTED POWER ($n_1 = 1.432$, $n_2 = 1.0$)

k_0d		0.5	1.0	2.0	4.0
$P^{T(1)}$	Guided	0.92325	0.97528	0.98732	0.90899
	Radiation	0.75691×10^{-1}	0.26752×10^{-1}	0.26601×10^{-2}	0.96803×10^{-1}
	Total	0.99894	1.00199	0.98998	1.00580
$P^{R(1)}$	Guided	0.14826×10^{-2}	0.32399×10^{-2}	0.21542×10^{-2}	0.31563×10^{-2} 0.68104×10^{-2}
	Radiation	0.17909×10^{-2}	0.13133×10^{-2}	0.12396×10^{-2}	0.86474×10^{-2}
	Total	0.32735×10^{-2}	0.45532×10^{-2}	0.33938×10^{-2}	0.18614×10^{-1}
$P^{T(1)}+P^{R(1)}$		1.00221	1.00654	0.99338	1.02441
$P^{T(2)}$	Guided	0.21357×10^{-5}	0.92822×10^{-5}	0.13693×10^{-4}	0.29406×10^{-4}
	Radiation	0.34411×10^{-5}	0.59777×10^{-5}	0.22633×10^{-4}	0.10180×10^{-2}
	Total	0.55768×10^{-5}	0.15260×10^{-4}	0.36326×10^{-4}	0.10475×10^{-2}
$P^{T(1+2)}$	Guided	0.92149	0.96936	0.99343	0.90026
	Radiation	0.75208×10^{-1}	0.26092×10^{-1}	0.31076×10^{-2}	0.81402×10^{-1}
	Total	0.99670	0.99545	0.99654	0.98166
$P^{T(1+2)}+P^{R(1)}$		0.99997	1.00000	0.99994	1.00028

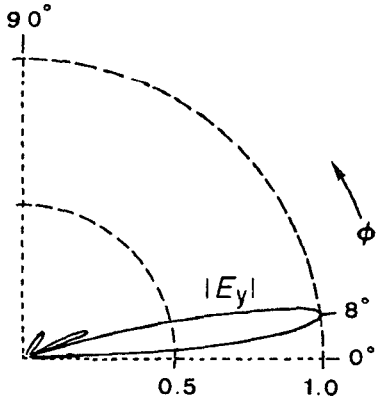

Fig. 4. Far radiated electric field pattern ($n_1 = 1.01$, $n_2 = 1.0$, $k_0d = 20.0$).

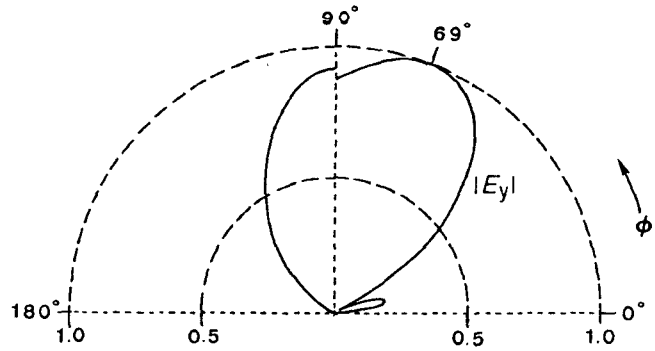

Fig. 5. Far radiated electric field pattern ($n_1 = 1.432$, $n_2 = 1.0$, $k_0d = 2.0$).

TABLE III
FIRST-ORDER REFLECTED AND TRANSMITTED POWER ($n_1 = 1.502$, $n_2 = 1.5$, $k_0 d = 6\pi$)

θ (Bent Angle)		1°	2°	3°
$P^{T(1)}$	Guided	0.86258	0.56434	0.29187
	Rad. (even)	0.13036×10^{-1}	0.11120	0.26131
	Rad. (odd)	0.12439	0.32446	0.44682
	Total	1.00000	1.00000	1.00000
$P^{R(1)}$	Guided	0.15912×10^{-14}	0.19736×10^{-13}	0.63180×10^{-13}
	Rad. (even)	0.30512×10^{-7}	0.46961×10^{-6}	0.19819×10^{-5}
	Rad. (odd)	0.16348×10^{-4}	0.34647×10^{-4}	0.33690×10^{-4}
	Total	0.16379×10^{-4}	0.35117×10^{-4}	0.35671×10^{-4}
$P^{T(1)} + P^{R(1)}$		1.00002	1.00004	1.00004
θ (Bent Angle)		4°	5°	10°
$P^{T(1)}$	Guided	0.12326	0.42511×10^{-1}	0.18270×10^{-3}
	Rad. (even)	0.38090	0.45073	0.49972
	Rad. (odd)	0.49584	0.50676	0.50010
	Total	1.00000	1.00000	1.00000
$P^{R(1)}$	Guided	0.95456×10^{-13}	0.67899×10^{-13}	0.67785×10^{-12}
	Rad. (even)	0.45116×10^{-5}	0.10308×10^{-4}	0.47658×10^{-3}
	Rad. (odd)	0.34514×10^{-4}	0.88099×10^{-4}	0.21157×10^{-3}
	Total	0.39025×10^{-4}	0.98407×10^{-4}	0.68816×10^{-3}
$P^{T(1)} + P^{R(1)}$		1.00004	1.00010	1.00069

values are listed in Table I for the four cases of $k_0 d = 5.0$, 10.0, 20.0, and 40.0 with $n_1 = 1.01$ and $n_2 = 1.0$ and in Table II for the four cases of $k_0 d = 0.5$, 1.0, 2.0, and 4.0 with $n_1 = 1.432$ and $n_2 = 1.0$. The symbols $P^{T(1)}$ and $P^{R(1)}$ indicate the first-order transmitted and reflected power, respectively; $P^{T(2)}$ indicates the power of the second-order transmitted field, while $P^{T(1+2)}$ indicates the power of the sum of the transmitted field up to the second-order, which is different from $P^{T(1)} + P^{T(2)}$. Although results with higher accuracy would be obtainable, up to the five significant figures are shown in the tables. Two guided modes can be guided only in the case of $k_0 d = 40.0$ for the examples of Table I and only in the case of $k_0 d = 4.0$ for the examples of Table II; all others are the single guided mode waveguides.

It is observed that in the case where the difference between core and cladding refractive indices is very small, as in the examples in Table I, the reflected power is extremely small and the second-order transmitted power becomes even smaller. Therefore we can say that the calculation of only the first-order transmitted field suffices for a practical solution. Also, it is observed from Table II that even for the case of a relatively large difference between core and cladding refractive indices, calculation of the transmitted fields up to the second order is sufficient to attain very high accuracy; e.g., even in the worst case the relative error in the energy relation is less than 0.03%.

Far radiated fields can easily be obtained by applying the method of steepest descents to the radiation mode expansion part of mode expansion expressions for the transmitted and reflected fields. Figs. 4 and 5 show a plot of the absolute value of far radiated first-order electric field $|E_y(\phi)|$ for the cases of $n_1 = 1.01$, $n_2 = 1.0$, $k_0 d = 20.0$ and $n_1 = 1.432$, $n_2 = 1.0$, $k_0 d = 2.0$, respectively. In Fig. 4, only the transmitted side is shown because the reflected side value is negligibly small. The small discrepancy observed at the 90° position in Fig. 5 is caused by a neglect of the higher order fields. Incidentally, it is confirmed for all eight cases that the first-order transmitted radiation power calculated from the following expression:

$$P = 2\int_0^{\pi/2}\left(\frac{1}{2}\sqrt{\frac{\epsilon_2}{\mu_2}}\,|E_y(\phi)|^2\right) n_2 k_0 r\, d\phi \qquad (38)$$

using discretization every 1° and the same power calculated from another expression,

$$P = \int_0^{n_2 k_0} |b(\Gamma)|^2\, d\Gamma \qquad (39)$$

agree to within 1.5%.

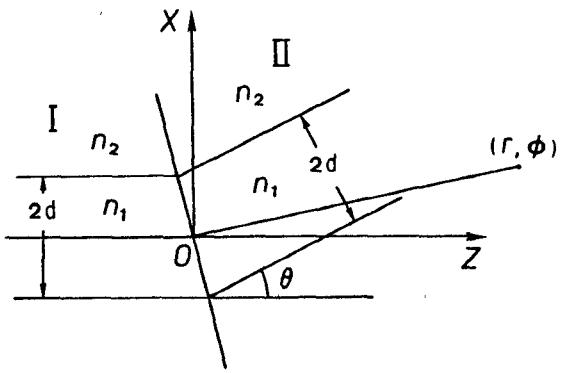

Fig. 6. Sharp bend.

B. Sharp Bends

Another discontinuity configuration examined numerically is the sharp bend shown in Fig. 6. The bent angle is θ and the core width is the same for waveguides I and II.

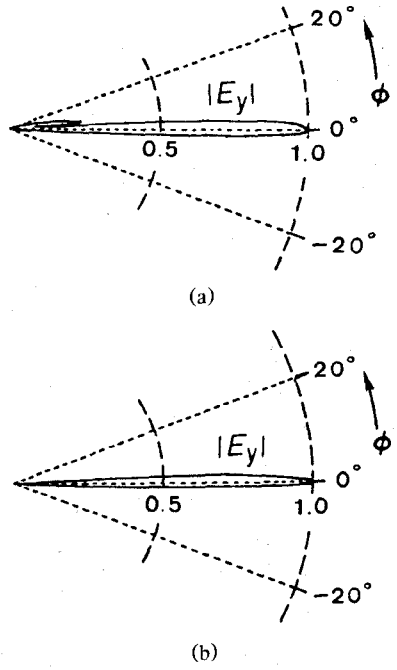

Fig. 7. Far radiated electric field pattern ($n_1 = 1.502$, $n_2 = 1.5$, $k_0 d = 6\pi$): (a) $\theta = 4°$; (b) $\theta = 20°$.

Again, the incident field is assumed to be the TE_0 mode field with unit power. The first-order reflected and transmitted power values are shown in Table III for the six cases of bend angle $\theta = 1°$, 2°, 3°, 4°, 5°, and 10° with $n_1 = 1.502$, $n_2 = 1.5$, and $k_0 d = 6\pi$. As seen from Table III, the first-order reflected guided mode power is less than 10^{-10} for all cases, which means that the reflected guided mode power is insignificant. It is seen that the reflected radiation power is also very small. Therefore, we can say that full-wave analysis including reflected fields is unnecessary for sharp bends as long as the bend angle is not too large.

Parts (a) and (b) of Fig. 7 show the far radiated electric field $|E_y|$ for the cases of $\theta = 4°$ and 20°, respectively. Incidentally, the far-field pattern for $\theta = 10°$ also was found to become much the same as that for $\theta = 20°$.

IV. Conclusions

An analytical and successive method for solving electromagnetic fields in abrupt discontinuities of dielectric slab waveguides has been presented and numerical results shown for step discontinuities and sharp bends. The results can serve as data for checking the accuracy of solutions obtained using other numerical techniques that would be useful for solving more complicated discontinuity configurations. Although the present method is particularly effective when applied to abrupt discontinuities in open type waveguides, where the reflected power is very small, the method is also applicable, theoretically, to discontinuity configurations causing large reflected power. Moreover, the method could easily be extended to problems of abrupt discontinuities of any type of waveguides, including closed types.

References

[1] P. Gelin, M. Petenzi, and J. Citerne, "Rigorous analysis of the scattering of surface waves in an abrupt ended slab dielectric waveguide," *IEEE Trans. Microwave Theory Tech.*, vol. MTT-29, pp. 107–114, Feb. 1981.

[2] T. Nobuyoshi, N. Morita, and N. Kumagai, "Scattering and mode conversion of guided modes by an arbitrary cross-sectional cylindrical object in an optical slab waveguide," *J. Lightwave Technol.*, vol. LT-1, pp. 374–380, June 1983.

[3] C. N. Capsalis, J. G. Fikioris, and N. K. Uzunoglu, "Scattering from an abruptly terminated dielectric-slab waveguide," *J. Lightwave Technol.*, vol. LT-3, pp. 408–415, Apr. 1985.

[4] K. Hirayama and M. Koshiba, "Analysis of discontinuities in an open dielectric slab waveguide by combination of finite and boundary elements," *IEEE Trans. Microwave Theory Tech.*, vol. 37, pp. 761–768, Apr. 1989.

[5] D. Marcuse, *Theory of Dielectric Optical Waveguides*. San Diego: Academic Press, 1974.

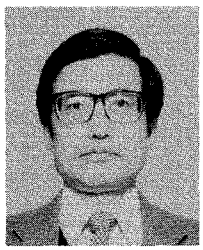

Nagayoshi Morita (M'67–SM'84) received the B.S., M.S., and D.Eng. degrees in communication engineering from Osaka University in 1964, 1966, and 1977, respectively.

From 1966 to 1991, he was with the Department of Communication Engineering, Osaka University, Japan. From September 1979 to June 1980, he was in Denmark on a research scholarship. In April 1991, he became a Professor in the Department of Electrical Engineering at the Chiba Institute of Technology, Narashino, Chiba, Japan. His work has included millimeter and optical waveguides, analytical and numerical techniques for electromagnetic wave problems, and hyperthermia. He coauthored the books *Electromagnetic Waves and Boundary Element Methods* and *Analysis Methods for Electromagnetic Waves*.

Dr. Morita is a member of the Institute of Electronics, Information, and Communication Engineers of Japan, the Japan Society of Medical Electronics and Biological Engineering, and the Japanese Society of Hyperthermic Oncology.